Astron. Astrophys. 344, 7–16 (1999)

ASTRONOMY AND ASTROPHYSICS

Radiative ages in a representative sample of low luminosity radio galaxies

P. Parma[1], **M. Murgia**[1,5], **R. Morganti**[1], **A. Capetti**[2], **H.R. de Ruiter**[1,3], **and R. Fanti**[1,4]

[1] Istituto di Radioastronomia, CNR, Via Gobetti 101, I-40129 Bologna, Italy
[2] Osservatorio Astronomico di Torino, Strada Osservatorio 20, I-10025 Pino Torinese, Italy
[3] Osservatorio Astronomico, Via Zamboni 33, I-40126 Bologna, Italy
[4] Dipartimento di Fisica, Università di Bologna, Via Irnerio 46, I-40126 Bologna, Italy
[5] Dipartimento di Astronomia, Università di Bologna, Via Zamboni 33, I-40126 Bologna, Italy

Received 12 June 1998 / Accepted 6 November 1998

Abstract. Two frequency observations, mainly at 1.4 and 5 GHz from the VLA, have been used to study spectral variations along the lobes of some nearby low luminosity radio galaxies that constitute a representative sample selected from the B2 catalogue. The variations of the spectral index have been interpreted as being due to synchrotron and inverse Compton losses and characteristic spectral ages are deduced for the relativistic electrons. The *radiative ages* are in the range of several 10^7 years. These *ages* correlate well with the source sizes. They also appear to be consistent with *dynamical ages* determined from ram-pressure arguments, if we make reasonable assumptions about the ambient gas density and allow for very moderate deviations from the equipartition conditions. There appears to be a significant difference between the radiative ages of sources in our sample and those of more powerful 3CR radio sources. We briefly discuss the possibility of re-acceleration processes and indicate some objects where these may occur.

Key words: radio continuum: galaxies – galaxies: active

1. Introduction

The determination of ages of extragalactic radio sources is one of the key points for any theoretical model that wants to explain their origin and evolution. As the radiation is due to the synchrotron process by relativistic electrons spiraling in magnetic field, much of the effort in determining source ages goes into the study of the radio spectra, for which the synchrotron theory predicts a frequency break due to the radiative energy losses, which drifts in time. According to various source evolution models, relativistic electrons in different regions of the source are deposited there at different times, so that the frequency break effectively is a clock that indicates the time elapsed since their production.

For several years spectral studies were based on the integrated spectrum of the radio sources (see e.g. Kellerman 1964; van der Laan & Perola 1969). The advent of high resolution interferometric systems, like the Cambridge 5-km Telescope, the Westerbork Synthesis Radio Telescope (WSRT) and the Very Large Array (VLA), has made it possible to study the spectral behaviour in different regions of a source. For a limited number of objects, detailed studies of the radio spectra across the emitting regions (see e.g. Alexander 1987; Carilli et al. 1991; Feretti et al. 1998) have produced break frequency maps and, from them, source age maps. However, in the majority of these studies the radio spectra across a source are based on only one pair of frequencies, so that the break frequency cannot be seen directly from the data. Nevertheless, with some additional assumptions which find their justification from the results obtained from the well studied objects, the break frequency can be estimated with reasonable accuracy. In fact, the large body of data now available in literature is obtained in this way (see e.g. Alexander & Leahy 1987; Leahy et al. 1989; Liu et al. 1992, for a large set of data on powerful 3CR sources).

Recently more sophisticated methods of analyzing spectral maps have been developed by Katz-Stone et al. (1993), Katz-Stone & Rudnick (1994) and Rudnick et al. (1994). These authors point out that the traditional method may lead to misinterpretation. In addition, Eilek & Arendt (1996) consider synchrotron spectra arising from a distribution of magnetic field strength and show that high frequency steepening of the spectrum need not necessarily be due to synchrotron ageing. Nevertheless we follow here the traditional spectral analysis, since this will facilitate comparison with the bulk of the literature in which this kind of analysis is very common. Moreover, the limited quality of our data does not allow anything more sophisticated.

Alternative methods for age determination are based on dynamical arguments, in particular the balance between the jet thrust and the ram-pressure due to the external medium (see e.g. Carilli et al. 1991 for Cygnus A). There is some debate about the consistency of the results between the two methods (see again Carilli et al. 1991 and Eilek 1996).

In this paper we present a two frequency spectral study of a representative subsample of the B2 radio galaxies and discuss ra-

Send offprint requests to: P. Parma

diative ageing of the relativistic electrons caused by synchrotron and inverse Compton (I.C.) energy losses. The present study is complementary to those quoted above, which deal with powerful 3CR radio sources: the B2 radio sources are less powerful by about two orders of magnitude[1].

The data on which this work is based and the spectral properties are described in Sects. 2 and 3. In Sect. 4 we briefly outline a possible interpretation of the results in terms of radiation theories. In Sect. 5 radiative ages are compared with those derived from dynamical arguments and we discuss how the two estimates can be made mutually consistent. We also compare the results based on our sample with those obtained for more powerful radio sources and discuss the differences we find. Finally, we comment on the possible occurrence of particle re-acceleration.

2. Source selection and spectral data

The B2 sample of radio sources, which contains about a hundred objects, was obtained from identification of B2 radio sources with bright elliptical galaxies (see Colla et al. 1975; Fanti et al. 1978). Because of the selection criteria, the sample is dominated by radio galaxies with a power typically between 10^{23} and 10^{25} WHz^{-1} at 1.4 GHz. Most are FRI sources. A few have a Head-Tail (HT) or Wide-Angle-Tail (WAT) structure, or are 3C31-like objects, i.e. sources whose brightness fades gradually with distance from the core. The majority, however, are double sources with bright symmetric jets, while hot-spots are usually weak or even absent. The sample has been extensively studied with different VLA configurations at 1.4 GHz (see references in Fanti et al. 1987). More recently Morganti et al. (1997a) observed 56 sources of the sample at 5 GHz, 25 with D array, 21 with C array and 10 with B array. These observations match the resolution of previous 20 cm observations and were originally planned in order to study depolarization asymmetries (Morganti et al. 1997b) in the lobes at a moderate resolution.

From the above sample we have selected sources which fulfil the following criteria:

a) a ratio of overall source size to beam size $\gtrsim 10$;
b) a signal to noise ratio per map point > 5, at both frequencies, for at least 8 independent slices, separated by at least one beamwidth, and perpendicular to the source axis, in order to obtain a trend of the spectrum along the source.

This leaves us with 32 sources of the original sample. Of these, 29 have double lobed morphology, 2 are WATs and 1 is a NAT. Due to criterion a), these sources tend to be the ones with larger angular and linear size. For some objects a spectral analysis had already been done in the past (Morganti et al. 1987; Capetti et al. 1995). However, these data have been re-analyzed here in order to ensure homogeneity.

We have carefully checked if the maps account for the total flux density (as measured by lower resolution observations), in order to avoid spurious spectral trends due to missing flux at one of the two frequencies or even at both. The VLA fluxes and those at lower resolution generally agree within the combined error, except for a few sources which were therefore excluded from the following analysis.

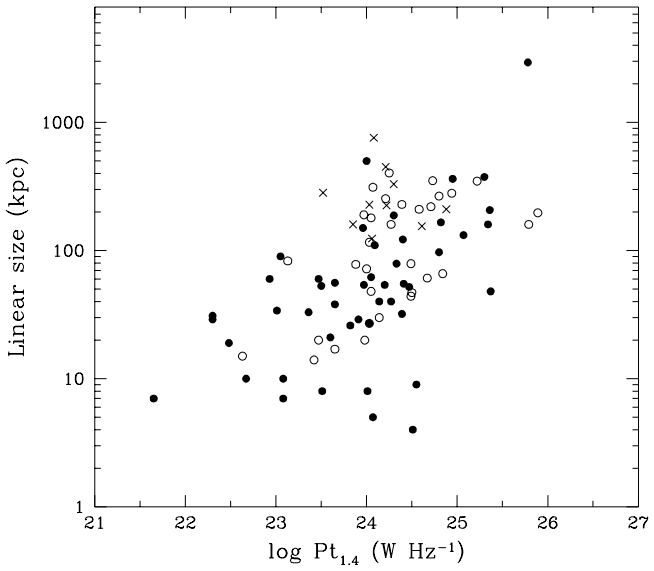

Fig. 1. Linear size as a function of radio power (at 1.4 GHz). Open circles: sources with spectral index calculated from VLA data; crosses: sources with spectral index taken from the literature; filled circles: B2 sources for which no spectral index information is available.

Fig. 1 shows how the sources of the B2 subsample (with spectral index information[2] either presented here or available in the literature; see below) are distributed in the radio power—linear size plane, and how this compares with the complete B2 sample. Clearly, for linear sizes larger than 10 kpc the subsample can be considered to be representative of the complete B2 sample.

For each source we have found the average of the two frequency spectral index $\alpha_{5.0}^{1.4}$ for slices perpendicular to the source axis and thus produced the variation of the spectral index along the source major axis. The slices are one beam across, so that the data points are practically independent. By visual inspection of the intensity maps we decided which source regions containing radio jets and hot spots were to be excluded.

Spectral index errors along the profiles are largely determined by the map noise and in a minority of cases by dynamic range. They are typically ≈ 0.05, but can be as high as ≥ 0.1 in the faintest regions considered. Unfortunately the cut-off imposed on brightness at 5 GHz introduces a bias against the inclusion of regions with very steep spectra. Possible cases of such steep-spectrum emission are noted in Sect. 3.

In most objects the spectral index clearly varies with distance from the core. The spectrum either steepens from the lobe outer edge inward (hereafter referred as "spectral type 2"; see 0908+37 in Fig. 2), or from the core outward ("spectral type 1"; see 1621+38 in Fig. 2). Only a minority of sources does not show any significant spectral index trend (these are given as spectral type 3 in Table 1). In Fig. 3 we show the behaviour of

[1] We use $\mathrm{H}_0 = 100$ km s^{-1}Mpc^{-1}

[2] We use the convention $S \sim \nu^{-\alpha}$

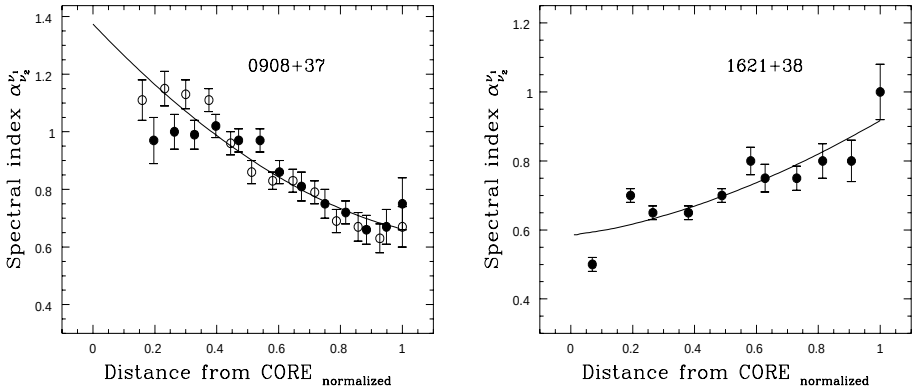

Fig. 2. Two examples of the spectral index distribution as a function of distance from the core. The distances are normalized to the maximum extent of a lobe. 0908+37 is a double lobed source and the filled and open circles refer to the two lobes. 1621+38 is a NAT source. The full lines are the best fit of the radiative model described in the text.

Table 1. Source parameters

B2 name	α_{max}	$\nu_{\rm br-min}$ GHz	α_{inj}	B_{eq} μG	Age Myrs	LS kpc	LS_n	$\log P_{1.4}$ WHz^{-1}	spectral type	FR type	
0034+25	1.3	4.4	0.63	2.5	67	83	3.30	23.13	2	I WAT	
0206+35	1.2	6.2	0.63	5.6	35	47	0.42	24.50	2	I	
0755+37	0.75	>30.0	0.71	4.4	<19	79	0.53	24.49	3	I	
0828+32	0.7	>25.0	0.48	2.3	<27	220	1.54	24.71	2	II	
0836+29	1.2	15.1	0.77	3.6	28	351	2.45	24.73	?	I-II	
0844+31	1.4	10.0	0.84	2.4	40	266	1.66	24.80	1	I-II	
0908+37	1.1	6.0	0.66	7.4	24	66	0.39	24.84	2	I-II	
0922+36	1.2	5.4	0.45	5.0	36	280	1.40	24.94	1	I-II	
1005+28	0.95	2.8	0.79	2.0	58	403	4.28	24.25	2	I-II	
1102+30	1.05	6.3	0.63	2.5	49	160	1.84	24.27	2	I	
1113+29	0.95	21.0	0.73	6.3	17	61	0.45	24.67	2	I-II	
1116+28	1.3	4.3	0.60	2.2	62	229	2.35	24.39	1	I WAT	
1254+27	1.4	7.7	0.66	5.0	35	15	0.94	22.63	1	I	
1322+36	0.75	>30.0	0.64	16.0	<4	14	0.41	23.42	3	I	
1347+28	0.8	11.6	0.56	7.3	18	48	0.71	24.05	2	I-II	
1357+28	0.85	>30.0	0.80	3.3	<22	116	1.76	24.03	3	I	
1422+26	0.9	14.4	0.66	4.5	28	72	1.03	24.00	2	I	
1441+26	1.05	3.0	0.72	2.3	75	190	2.88	23.97	2	I-II	
1455+28	0.8	>30.0	0.79	5.6	<13	348	1.74	25.22	3	II	
1521+28	1.0	17.5	0.72	3.0	28	210	1.52	24.58	1	I	
1525+29	1.0	18.3	0.78	9.0	12	20	0.30	23.98	2	I	
1528+29	1.2	17.7	0.87	2.2	29	254	3.76	24.21	1	I-II	
1609+31	0.65	21.2	0.54	9.6	10	30	0.39	24.14	2	I-II	
1613+27	0.75	>30.0	0.67	9.0	<9	27	0.26	24.03	3	I	
1615+32	1.6	3.0	0.62	5.7	41	160	0.76	25.79	2	II	3C 332
1621+38	0.9	14.6	0.59	9.8	12	17	0.39	23.65	1	I NAT	
1626+39	2.1	0.56	0.59	10.4	$57_{\rm KP}$	44	0.37	24.49	1	I	3C 338
1643+27	0.8	16.7	0.52	5.2	20	180	2.55	24.05	1	I-II	
1658+30	0.9	8.4	0.59	2.8	46	78	1.42	23.88	2	I-II	
1726+31	1.3	6.5	0.67	7.0	23	197	0.99	25.89	2	II	3C 357
1827+32	1.3	6.4	0.48	1.8	50	312	4.00	24.07	1	I	
2236+35	0.9	11.7	0.61	8.0	17	20	0.56	23.47	?	I	

Column 1: Source name in the B2 catalogue, with reference to 1950 coodinates; 2: larger observed spectral index; 3: minimum break frequency, from the fit; 4: assumed injection spectral index; 5: equipartition magnetic field; 6: source age, from the JP model (except for 1626+39); 7: source linear size; 8: source size, normalized to the median value for its radio luminosity; 9: radio luminosity; 10: spectral class (see text); 11: Fanaroff-Riley type, taken from Morganti et al. (1997b); 12: 3C name.

the spectral index separately for type 1 and type 2 sources. The ultra-steep source B2 1626+39 is the only one not used in Fig. 3.

From a literature search we were able to recover additional information on the spectral index distribution, for 15 objects in

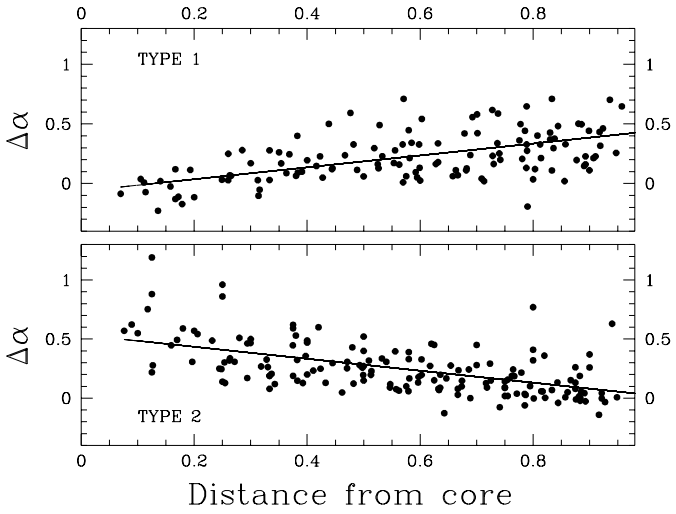

Fig. 3. $\Delta\alpha = \alpha - \alpha_o$ as a function of distance from the core, for type 1 and type 2 sources. For the definitions of α_o and spectral type see the text. The distance from the core is normalized to the lobe extent. The data of all sources except B2 1626+39 were used.

the B2 radio galaxy sample. Their spectral data generally come from frequency pairs other than 1.4/5 GHz. We have re-analyzed these data with criteria similar to ours and using the same ageing model (JP, see Sect. 4), in order to ensure as much as possible homogeneity. The data are reported in Table 2 and individual notes are given in the next section. The meaning of the columns is as for Table 1.

Four of these sources also belong to our VLA sample; in Sect. 3 we comment on the spectral ages derived from the different sets of data.

3. Notes on individual sources

0034 + 25. The source is a WAT. The spectral index is well sampled in the eastern arm only, which is straight. The south-western arm, which is strongly bent, has a lower brightness, so that the spectral index can be measured only in a few areas close to the outer edge.

0055 + 30. This is a well studied radio galaxy. However the spectral properties of this source are still contradictory. Jägers (1981) gives a spectral index profile along the source (between 0.6 and 1.4 GHz), which shows a clear steepening outwards, but also large fluctuations are visible. The average trend would indicate a minimum break frequency ≥ 1.6 GHz and a maximum source age $\approx 10^2$ Myrs. Mack et al.(1998), based on multifrequency data including Effelsberg 10.5 GHz, compute the spectrum in various areas and find large fluctuations from region to region. They estimate ages ≤ 12 Myrs. We favour the longer timescale, although we feel that the situation is rather uncertain.

0828 + 32. The radio source has a cross shaped structure with two prominent low brightness wings almost perpendicular to the much brighter lobes (Parma et al. 1985). The source has been discussed in terms of precession (see also Klein et al. 1995). Our VLA data allow us to study the brighter lobes only, which do not show any clear steepening (consistent with what was found by Parma et al. 1985). The wings have much steeper spectra (Parma et al. 1985; Klein et al. 1995). The source age in Table 1 refers to the bright lobes, while the one in Table 2 is obtained from the spectral steepening in the wings.

0836 + 29. The source shows a clear spectral steepening in the western tail of the southern lobe, which begins at the hot spot position and is almost perpendicular to the source main axis. The spectral index may go up to 1.5 (as considered in Capetti et al. 1995), but in the present analysis we have considered only areas where the signal to noise ratio is > 5: we excluded therefore the steeper spectrum areas. The northern lobe is so small that it is impossible to follow any spectral trend. Besides our 1.4/5 GHz VLA data (Table 1), the source spectrum has been studied with different resolution in the frequency range 0.6/10.5 GHz (Table 2). The source ages determined from the two different frequency ranges are in reasonable agreement.

0844 + 31. The source was studied by Capetti et al. (1995). Both lobes contain hot spots. The spectrum steepens from the hot spots outward. In the southern lobe, the spectral index appears to reach a saturation value, after an initial steepening. The same may happen in the northern lobe. This behaviour is discussed in terms of re-acceleration processes in Sect. 5.4.

0922 + 30. The spectrum of the southern lobe steepens outwards from a hot spot, which is located well inside the lobe. The northern lobe is too small to be able to see any spectral trend.

0924 + 30. See also Cordey (1987), for a discussion of this source, which is believed to be a remnant.

1005 + 28. The spectrum steepens inward in the lobes. However, due to the low brightness of the source, we can follow the spectral steepening only for about half the length of the lobes. The estimated age is derived by extrapolating the observed spectral trend back to the core.

1116 + 28. The source is a WAT. The radio spectrum steepens away from the radio core and seems to saturate at about 2/3 of the arms' length. This behaviour is discussed in terms of re-acceleration processes in Sect. 5.4.

1441 + 26. See note for 1005+28.

1521 + 28. See Capetti et al. (1995). The southern lobe is very long and contains a weak hot spot in the middle, from where the spectral index increases outwards and then saturates at a constant value. This behaviour is discussed in terms of re-acceleration processes in Sect. 5.4. No spectral trend can be followed in the northern lobe, which is too small.

1528 + 29. The source has a double lobed morphology with rather bright twin jets. The spectrum steepens outwards and seems to saturate at about half lobe length. This behaviour is discussed in terms of re-acceleration processes in Sect. 5.4.

1615 + 35. This is a NAT source. Ekers et al. (1978b) show that the spectral index, after an initial steepening, saturates at $\approx$ 1.1.

1621 + 38. The source is a small NAT.

1626+39. The radio spectrum is very steep all over the source, perhaps slightly steeper in the outer regions. The JP model is

Table 2. Sources taken from the literature

B2 Name	Freq. range	Age Myrs	$\log P_{1.4}$ WHz^{-1}	LS kpc	LS_n	Spectral type	Ref.	FR type	
0055+30	0.3/0.6	112	24.08	760	17.9	1	1	I	NGC315
	0.6/1.4						9		NGC326
0055+26	1.4/5	35	24.61	155	1.2	2	2	I	
0104+31	2.7/5	93	24.21	450	4.9	1	3	I	3C 31
	0.6/1.4						9		
0326+39	0.6/1.4	64	24.06	124	2.1	2	4	I	
	0.6/11						6		
0828+32	0.6/1.4	59	24.71	220	1.5	2	5	II	
	0.6/11						6		
0836+29	0.6/1.4	30	24.73	351	2.4	?	6	I-II	
0844+31	0.6/1.4	<35	24.80	266	1.6	1	9	I-II	
0924+30	0.6/1.4	69	23.52	283	7.3	2	10	II	
	0.6/11						11		
1243+26	0.6/11	39	24.23	129	2.3	1	6	I	
1321+31	0.6/11	35	23.85	160	3.4	2	6	I	
1358+305	0.3/1.4	62	25.27	1330	9.1	2	7	II	
1615+35	0.6/1.4	78	24.30	330	3.7	1	8	I	
	0.6/11						6		
1827+32	0.6/11	>30	24.07	312	4.0	1	6	I	
2229+39	0.4/2.7	74	24.03	228	3.1	1	3	I	3C 449
	2.7/5						3		
	0.6/1.4						9		
2335+26	0.6/1.4	60	24.88	210	1.2	1	9	I	3C 465

References: 1) Mack et al. (1998); 2) Ekers et al. (1978a); 3) Andernach et al. (1992); 4) Bridle et al. (1991); 5) Parma et al. (1985); 6) Klein et al. (1995); 7) Parma et al. (1996); 8) Ekers et al. (1978b); 9) Jägers (1981); 10) Ekers et al., 1981; 11) Klein et al., 1996

unable to fit the spectral index distribution, while the KP model is rather satisfactory. The age in Table 1 is from this last model. An alternative and physically more acceptable fit is discussed in Sect. 5.4. The source is associated with the brightest galaxy of the cluster A 2199.

$2236+35$. The source shows two faint wings, antisymmetric with respect to the main bright lobes. The spectrum in the bright lobes is almost constant ($\alpha_{5.0}^{1.4} \approx 0.6$). However a clear spectral steepening is seen in the eastern wing. The source age is derived from this steepening.

4. Determination of the radiative ages

4.1. The models and the assumptions

The spectral trends along the sources are interpreted in terms of radiative ageing of the relativistic electrons by synchrotron and I.C. processes. The analysis of the spectral data follows well known arguments (see, e.g. Myers & Spangler 1985). By assuming an injection spectral index, α_{inj}, it is possible to obtain the break frequency, ν_{br}, as a function of position along the source axis and, finally, for an assumed magnetic field, the age of the relativistic electrons in that position.

Theoretical synchrotron-loss spectra have been computed numerically (Murgia 1996) from the synchrotron formulae (e.g., Pacholczyk 1970). It is assumed that the synchrotron and I.C. losses dominate and that expansion losses and re-acceleration processes can be neglected (see e.g. Alexander 1987, for a discussion of synchrotron losses versus adiabatic expansion).

Two models are generally considered: i) the Jaffe-Perola (JP) model (Jaffe & Perola 1974), in which the time scale for continuous isotropization of the electrons is assumed to be much shorter than the radiative time-scale; ii) the Kardashev-Pacholczyk (KP) model (Kardashev 1962) in which each electron maintains its original pitch angle. We have preferred the JP model (except for 1626+39, see note) since the I.C. energy losses due to the microwave background radiation are as important as the synchrotron losses, and in the former random orientations are expected between electrons and photons.

The two frequency spectral index $\alpha_{\nu_2}^{\nu_1}$ allows us to compute the break frequency, ν_{br}, in various regions of the source, using the synchrotron-loss spectrum for the JP model. The break frequency is used to determine a spectral age, based on the formula:

$$t_s = 1.61 \times 10^3 \frac{B^{0.5}}{(B^2 + B_{CMB}^2)(\nu_{br}(1+z))^{0.5}}$$

where the synchrotron age t_s is in Myrs, the magnetic field B is in μG, the break frequency ν_{br} in GHz and $B_{CMB} = 3.2 \times (1+z)^2$ μG is the equivalent magnetic field of the cosmic microwave background radiation. It is assumed that the magnetic field strength is uniform across the source and has remained constant over the source life.

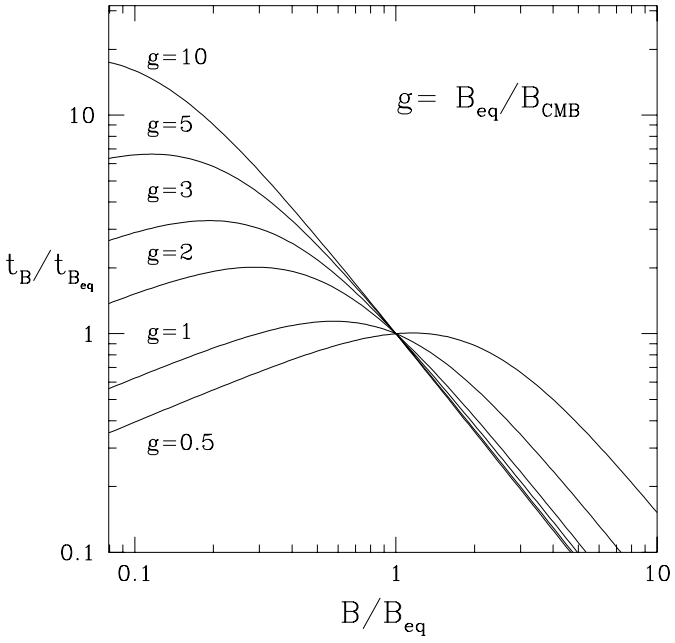

Fig. 4. The radiative lifetime as a function of the ratio B/B_{eq}.

The magnetic field is computed using the "minimum energy assumption". We assumed equality in the energy of protons and electrons, a filling factor of unity, a radio spectrum ranging from 10 MHz to 100 GHz and an ellipsoidal geometry. For most of the objects in our sample the computed magnetic field is within a factor 2 of B_{CMB}. This ensures that the synchrotron ages t_s are relatively independent of moderate deviations from the "minimum energy conditions".

Fig. 4 shows how the radiative life time depends on the ratio B/B_{eq}. For $0.5 < B_{eq}/B_{CMB} < 2$, deviations from equipartition have a small effect on the computed lifetime if $B \lesssim 2 \cdot B_{eq}$.

4.2. Spectral analysis

For the majority of the sources the quality of spectral information is comparable in the two lobes, and the spectral trends are rather similar when the errors are taken into account. Therefore we preferred to analyze the two lobes together, instead of considering them separately. We did this by folding the spectral profiles of the two lobes onto each other, after having normalized the coordinates along the lobe axis to the maximum lobe extent (as shown in Fig. 2, for 0908+37). We fitted the folded spectral index plots along the source axis (as in Sect. 2) with a relationship of the type:

$$\nu_{br} \propto x^{-2}$$

where x is the normalized distance from the outer lobe edge or from the core according to the observed steepening trend (as shown in Fig. 2). The above law is expected on the basis of the relation between radiative age and break frequency, if x is proportional to time, i.e. assuming a constant expansion speed. From it we obtain a best estimate of α_o, i.e. the spectral index close to the outer edge of the lobe or close to the core, according to the observed spectral profile. This, with a few exceptions discussed below, is assumed to be equal to the injection spectral index, α_{inj}. We find a mean value of $\alpha_o \approx 0.65$, with a dispersion ≈ 0.1. In this way we obtain from the folded spectral profiles the variation of the break frequency as a function of position, averaged over the two lobes. Extrapolating it to the inner or outer part of the source, we then obtain the "minimum break frequency", ν_{br-min}, namely the break frequency of the oldest electrons, that we use for determination of the source age. For the large majority of the sources the extrapolation introduces only minor additional uncertainties. The computed values of ν_{br-min} range from a few GHz up to several tens of GHz.

Considering the errors in the spectral index ($\gtrsim 0.05$) and the uncertainty in α_{inj} ($\lesssim 0.1$), the uncertainty in ν_{br-min} can be quantified as:

$$\Delta\nu_{br}/\nu_{br} \lesssim 0.08 \cdot (\nu_{br}(GHz))^{0.5}.$$

This implies that only values of $\nu_{br-min} \leq 30$ GHz are significant, which is hardly surprising given that our highest frequency is a factor six lower. The errors on t_s, for a given magnetic field, are $\approx$ 15%, for break frequencies of a few GHz, increasing up to $\geq$ 40% for break frequencies $\approx$ 30 GHz. Had we used the KP model, t_s would be shorter by ≈ 10 %.

As our analysis of the folded spectra might have missed some information on possible differences between the two lobes, we have further compared for each source the best fit model with the two lobes separately, in order to see how well each of them individually fitted the model. Differences between the two lobes appear to be insignificant. The α_o values of the two lobes are in general within 0.1 and the values of t_s are within the estimated uncertainties.

We have also performed a fit with a relationship $\nu_{br} \propto x^{-m}$, as a check of the assumption of constant expansion speed. Within the uncertainties, we find that m is close to two. We do not claim that the expansion speed is constant, but only state that our data do not show strong deviations from it.

We comment a bit more on α_{inj}, since ν_{br-min} strongly depends on it. Alexander & Leahy (1987) and Leahy et al. (1989), in their spectral study of several tens of 3CR radio sources, have used as α_{inj} the low frequency spectral index, α_{low}, of the integrated spectrum. For our sources this choice is less appropriate, since α_{low} (known between 0.4 and 1.4 GHz) has errors ≥ 0.1: therefore we prefer to use α_o. Nevertheless we have compared the α_o with the α_{low} in order to check consistency. For most sources α_o and α_{low} are the same within the expected errors. However, for sources which have $\nu_{br-min} < 10$ GHz, α_{low} tends to be systematically larger than α_o, by ≈ 0.1 or more. It appears that the integrated spectral index α_{low}, even when measured at low frequencies, has already suffered somewhat from radiative losses and therefore it is better to assume that $\alpha_{inj} = \alpha_o$. For two sources (0034+25, 0206+35) $\alpha_o \approx 0.9$–1.0, significantly different from α_{low} (≈ 0.6). For them we assume that α_o is modified from α_{inj} by a high frequency break, perhaps due to energy losses in the jet, and assume $\alpha_{inj} = \alpha_{low}$.

The radiative lifetimes are in the range of 10^7–10^8 years. We stress that we cannot exclude the possibility that we have

missed source areas with steeper spectra. Therefore the t_s we give are lower limits on the source ages.

5. Discussion

5.1. Two classes of source

There appear to be two classes of source in our sample (spectral types 1 and 2), according to the run of the $\alpha_{5.0}^{1.4}$ along the source axis. This double behaviour was already pointed out some time ago by Jägers (1981). In the "spectral type 2" sources, $\alpha_{5.0}^{1.4}$ increases from the outer edges of the lobes towards the core. Therefore the older electrons are found closer to the core. This class contains essentially sources with double lobed morphology, of both FR I and FR II type. Their spectral behaviour is that expected on the basis of standard source models where the radiating particles are deposited at different times at the end of an advancing beam and remain in that position or flow back at some speed toward the core. In this model the closer to the core the older they are.

In the "spectral type 1" the spectral index steepens away from the core. This class is known to contain "3C 31 like" objects, WATs, and NATs (see, e.g., Jägers, 1981). In our sample of Table 1 the spectral class 1 objects are: one WAT, one NAT and some double sources with plumes or wings where this spectral behaviour is seen. In this last type of objects hot spots, if present, are seen well inside the lobes and the steepening of the spectrum starts from there. One double source with very bright twin jets and narrow lobes (1528+29) also belongs to this class.

The distributions of radiative ages, t_s, for the two spectral classes are very similar.

5.2. A comparison between spectral and dynamical ages

We have compared the synchrotron ages, t_s, with the dynamical ages, t_d, evaluated from simple ram-pressure arguments. The expansion velocity of the lobes is given by the relation:

$$v_{exp} \approx \left[\frac{\Pi}{A}\,\frac{1}{m_p n_e}\right]^{0.5}$$

where Π is the jet thrust and A is the size of the area over which it is discharged.

The most simplistic assumption is to identify the Π/A ratio with the hot spot pressure. However various authors have suggested that the thrust is likely to be applied over a wider area and therefore that the deduced velocities are overstimated (see, e.g.: Norman, 1993 and Massaglia et al., 1996, where differences of up to a factor 3 are shown). The most popular mechanism for accomplishing this is the Scheuer's "dentist drill" scenario (Scheuer 1982), according to which the jet direction fluctuates on short timescale compared to the age of the source. In order to reduce this problem, we use, the front surface minimum pressures of the lobes, $p_{eq,f}$, as the appropriate quantity for Π/A (Williams, quoted by Carilli et al., 1991).

The values we find are typically ≤ 4 times the average minimum lobe pressure.

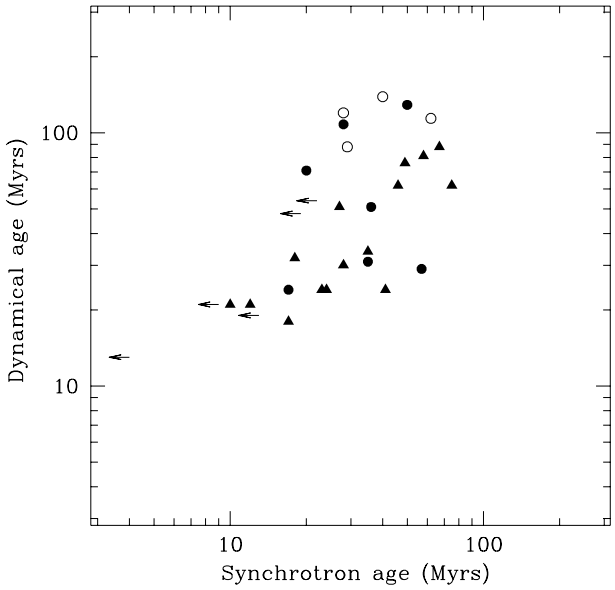

Fig. 5. Dynamical age vs spectral age of the source. For the meaning of the symbols see text.

We assume that the jet thrust is constant over the source life time and that the source grows in a self-similar way, such that $p_{eq,f} \propto R_{kpc}^{-2}$. Finally we assume a run of the external density $n_e = n_o \times R_{kpc}^{-\beta}$, with $n_o \approx 0.5\,\mathrm{cm}^{-3}$ and $1.5 \lesssim \beta \lesssim 2$, according to Canizares et al. (1987). Under these assumptions there would be only slight dependence, if any, of v_{exp} on source size, depending on the value of β.

We have excluded from this analysis the NAT source 1621+38, for which the ram-pressure model is likely to be incorrect. We have, instead, included the two WATs, although this may be questioned, since the jets are moderately bent in 1116+28 and one of them is straight in 0034+25, and they run undisrupted to the end of two lobes. In any case the exclusion of these two sources does not change our conclusions.

In Fig. 5 we show the plot t_s *vs* t_d, for $\beta = 2.0$. The dots represent sources with spectral type 1, the open circles referring to four sources which are discussed in Sect. 5.4 and whose radiative lifetimes could be definitely longer than the values given in Table 1. Sources with spectra of type 2 are denoted by triangles. The arrows refer to sources for which the t_s are upper limits.

The dynamical and radiative ages are correlated, but the dynamical ages in general are larger by a factor ≈ 4 for $\beta = 1.5$ and ≈ 2 for $\beta = 2$.

These discrepancies are believed to be not very serious for at least three reasons. First of all, the one-dimensional ram-pressure balance may not be realistic and discrepancies of a factor 2 or so are well possible, as mentioned above. Second, the central density we have assumed may be a bit too high. A value around $0.1\,\mathrm{cm}^{-3}$, which is not excluded by the X-ray data, would bring, for $\beta = 2$, the dynamical ages into closer agreement with the spectral ones. Third, the ram-pressure dynamical ages depend on the minimum energy assumption. It

has been shown that radio galaxies with luminosities like in the present sample usually have internal pressures larger than the minimum ones by a factor ≥ 5 (Morganti et al. 1988; Feretti et al. 1992). If we assume that the magnetic field is weaker than the one corresponding to minimum energy conditions by a factor ≥ 4, the internal pressure increases by a factor ≥ 4 and the dynamical lifetime decreases by a factor ≈ 2. Anyway, the radiative lifetimes would change little, as can be seen from Fig. 4. Likely both explanations may play a role in bringing t_s and t_d to a closer agreement.

5.3. Spectral ages and source sizes

We have investigated whether there is a relationship between radiative age and source size. We find a significant correlation between radiative age and linear size, as shown in Fig. 6. A linear fit between the logarithms of age and linear size gives:

$$LS \propto {t_s}^{0.97},$$

where the uncertainty in the exponent is 0.17.

The advance speed of the lobes, deduced from the synchrotron ages, are in the range of $0.5\text{–}5 \cdot 10^3$ km s^{-1}. There is no difference between the two spectral classes.

Alexander & Leahy (1987) have presented a strong correlation between the expansion speed, deduced from the radiative lifetimes, and radio power. Liu et al. (1992) comment also on this relation and point out that it could be caused partly by the assumption of $B = B_{eq}$. It should be noted that their sources are of spectral type 2. The velocities we have deduced from our sample, relatively independent of the equipartition assumption, are in good agreement with those of the low power sources in those samples.

5.4. Is there particle re-acceleration?

As mentioned in Sect. 4, we have analyzed our spectral data assuming that the dominant processes producing the energy losses of the relativistic electrons are synchrotron and inverse Compton, neglecting adiabatic expansion as well as re-acceleration. With the additional assumption of a constant advance speed of the source outer edges, this is the motivation for the fit to the spectral data, $\nu_{br} \propto x^{-2}$, that we have used in Sect. 4.2. The fits to the data in general are good, in the sense that they describe well the overall trend of $\alpha_{5.0}^{1.4}$ versus x.

There are however a few objects were the break frequency does not seem to increase always with x as expected from the simple synchrotron/I.C. model. An example is shown in Fig. 7.

The saturation of $\alpha_{5.0}^{1.4}$ to a constant value would indicate that the break frequency, after an initial decrease, does not decrease anymore. A possible explanation of this is that a re-acceleration process is acting, which compensates in part for the radiative energy losses and causes a freezing of the break energy at that value where the radiative and the acceleration time scales are equal. Of course, if re-acceleration processes are working, the ages estimated in the previous section would be underestimated.

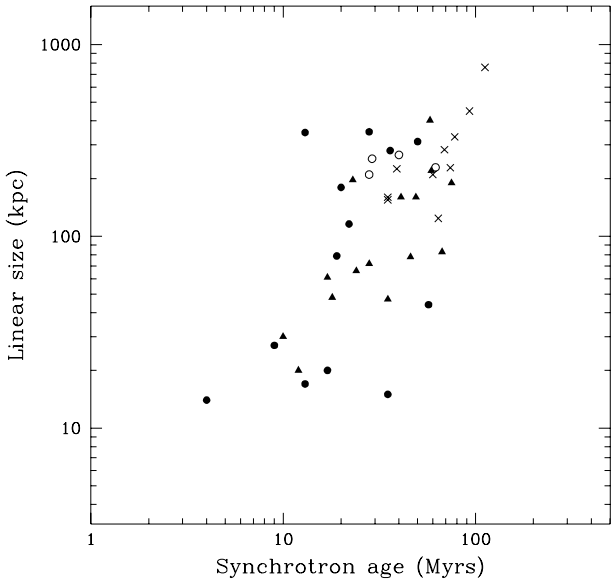

Fig. 6. Linear size as a function of spectral age of the source. The crosses represent the sources taken from the literature, the dots type 1 spectra, the open circles, as in Fig. 5, referring to the four sources discussed in Sect. 5.4. The triangles represent type 2 spectra.

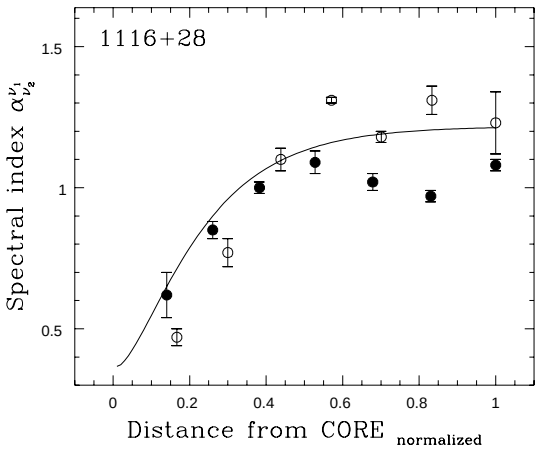

Fig. 7. Spectral index as a function of distance from the core, for the source B2 1116+28. The line represent the re-acceleration model described in the text.

Expressing the re-acceleration process as:

$$dE/dt = E/\tau_a,$$

where E is the particle energy, and τ_a is the acceleration time scale, the break frequency, as a function of time (see Kardashev, 1962), is given by:

$$\nu_{br} \propto \frac{B}{(B^2 + B_{CMB}^2)^2} \frac{1}{(1 - e^{-t/\tau_a})^2 \, \tau_a^2} \propto \frac{\rho^2}{(1 - e^{-\rho \, x})^2},$$

where ρ is the ratio of the source age to the re-acceleration time scale τ_a and x is the normalized distance from the outer lobe edge or from the core according to the observed steepening trend.

The above law naturally leads to a saturation of ν_{br} when $t \gtrsim \tau_a$.

We have re-fitted all the spectral profiles with the above formula and derived a value of ρ for each source and corresponding source age, t'_s, which is related to the previous ones, t_s by:

$$t'_s = \frac{t_s \rho}{1 - e^{-\rho}}$$

For at least 70% of the objects the results are not much different from the purely radiative model. For those we find $0 \leq \rho \leq 2$ (the median value is 1.1) and the lifetimes are modified by less than a factor 2. Time scales for re-acceleration must be typically $\geq 4 \cdot 10^7$ years.

However for a few sources (0844+31, 1116+28, 1521+28, 1528+29) we find $\rho > 5$, which suggests that re-acceleration may be present. Their ages would then be raised by factors from ≈ 6 to ≈ 10 with respect to the "radiation only" model. These objects seem to be among those where the spectrum steepens away from the core. Also 1626+39 is fitted reasonably well by this model and this is physically more acceptable than the KP model (see note in Sect. 3), but its age is only marginally modified.

Finally, we note that the possibility of re-acceleration processes is another factor which goes in the direction of bringing the radiative and the dynamical timescales closer.

5.5. Spectral ages and radio power: a comparison with the 3CR radio galaxies

We have compared the synchrotron ages derived for our sample with the corresponding ones for 3CR sources found by Alexander & Leahy (1987); Leahy et al. (1989) and Liu et al.(1992). When necessary the data were corrected, to take into account different assumed values for the Hubble constant.

Fig. 8 shows a plot of the ages versus radio power for the B2 and the 3C samples. It appears that the t_s of our sources are systematically larger than those of the 3CR sources by factors 5–10. In this context it is relevant to mention that Liu et al. (1992) noted that the synchrotron lifetimes of the more powerful 3CR sources are shorter than those of low-power sources. The trend of synchrotron age vs. radio power corresponds to a correlation between expansion speed and radio power, as recalled in Sect. 5.3, since the sizes of the sources in the two samples are not too dissimilar. There are several possible reasons for these differences, among which we mention the following.

a) As discussed by Liu et al. (1992), the radiative ages derived for the powerful sources (3CR) are heavily dependent on the equipartition magnetic field, B_{eq}, which is generally significantly larger than B_{CMB}. For B $\approx\ 1/4 \cdot B_{eq}$ the differences between the two sample would be greatly reduced.

b) Another possibility is that, if there is significant backflow in the powerful sources, in the inner regions there is an accumulation and mixing of the older electrons, with a consequent smoothing of the spectral break and an under-estimation of the maximum radiative time scale.

c) The effect could be real, namely in lower power sources, as those of our sample, the nuclear activity lasts for a longer time. One could think of an evolutionary effect, in the sense that low power sources have evolved from high power sources and are therefore older. We note, however, that the sources of our sample are on average smaller than powerful 3CR sources (de Ruiter et al. 1990), so that we consider this unlikely in general, even if it cannot be excluded as an explanation in some cases. Another possibility is a cosmological effect, since the 3CR sources are at much larger red-shifts than B2 radio galaxies.

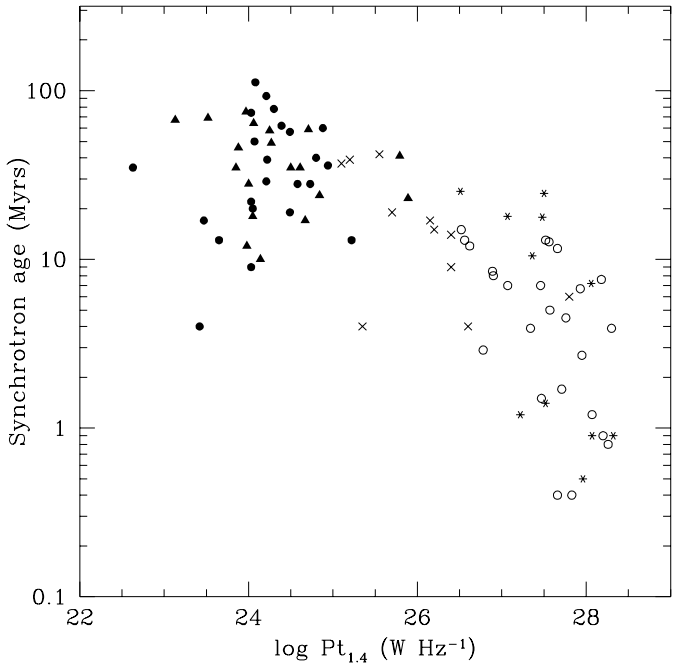

Fig. 8. Source age versus radio power at 1.4 GHz. The meaning of the symbols is as follows. Filled circles and triangles: B2 sources with type 1 and type 2 spectra, respectively; crosses: 3C galaxies with $z < 0.2$; open circles: 3C galaxies with $z > 0.2$; asterisks: 3C quasars.

We note that Scheuer (1995), based on an analysis of the lobe asymmetries of powerful radio sources, concluded that their growth rates are likely to be less than $0.1\ c$ and could be as low as $0.03\ c$. This would indicate source lifetimes that are longer than the radiative ones and closer to those we find for the B2 radio galaxies.

6. Conclusions

1) We have derived the variations of the spectral index across the source emitting regions for a representative sample of 32 radio galaxies from the B2 sample, by means of VLA maps at 1.4 and 5 GHz observations. From the literature we have found similar information for an additional 10 B2 radio galaxies, bringing the total number to 42. From these data, using a simple standard radiative ageing model, we have computed the radiative ages.

2) The typical ages we find are in the range of $10^7\ -10^8$ years, somewhat longer than the values found for more powerful 3CR radio sources. We discuss this point briefly and suggest that moderate deviations from the equipartition assumption, on which the age determination is based, may easily explain the discrepancy. However we cannot exclude that the effect is real.

3) We compare the radiative ages with dynamical ages obtained from a simple ram-pressure model. We find good statistical agreement between the two methods, for an average central gas density of the ambient medium ≈ 0.1 cm^{-3} and for moderate deviations from the equipartition conditions. A correlation is found between the linear size, LS, and the radiative age.

4) We discuss the possibility of re-acceleration of relativistic electrons in the source. A few objects appear to indicate the existence of such an effect. The time scale of re-acceleration is typically $\geq 4 \cdot 10^7$ years.

5) Our spectral interpretation is based on the generally assumed "standard model", namely an aged electron power law in a uniform magnetic field. In recent works this approch has been criticised (e.g. Katz-Stone et al., 1993; Eilek & Arendt,1996). It is claimed that high frequency spectral steepening is not necessarily due to synchrotron ageing. With our data we are not in a position to comment on these "non orthodox" views. Were they correct, the standard discussion of our data, as well as those made in the past, would be invalidated. However we feel that the reasonable agreement between the standard radiative ages and the dynamical ages from a simple ram-pressure model are suggestive that the standard picture is at least partly correct.

Acknowledgements. We are indebted to Drs. R. Laing and S. Spangler, who carefully read the manuscript and provided useful comments. We also thank the referee Dr. J. Riley, whose constructive criticism helped to improve the presentation of the paper. The National Radio Astronomy Observatory is operated by Associated Universities, Inc., under contract with National Science Foundation.

References

Alexander P., 1987, MNRAS 225, 27
Alexander P., Leahy J.P., 1987, MNRAS 225, 1
Andernach H., Feretti L., Giovannini G., et al., 1992, A&AS 93, 331
Bridle A.H., Baum S.A., Fomalont E.B., et al., 1991, A&A 245, 371
Canizares C.R., Fabbiano G., Trinchieri G., 1987, ApJ 312, 503
Capetti A., Fanti R., Parma P., 1995, A&A 300, 643
Carilli C.L., Perley R.A., Dreher J.W., Leahy J.P., 1991, ApJ 383, 554
Colla G., Fanti C., Fanti R., et al., 1975, A&AS 20, 1
Cordey R.A., 1987, MNRAS 227, 695
de Ruiter H.R., Parma P., Fanti C., Fanti R., 1990, A&A 227, 351
Eilek J.A., 1996, How Radio Sources Stay Young: Spectral Aging Revisited. In: Hardee P., Bridle A., Zensus J.(eds.) Proc. ASP Conference Series, Vol. 100, Energy Transport in Radio Galaxies and Quasars. p. 281
Eilek J.A., Arendt P.N., 1996, ApJ 457, 150
Ekers R.D., Fanti R., Lari C., Parma P., 1978a, Nat 276, 588
Ekers R.D., Fanti R., Lari C., Ulrich M.H., 1978b, A&A 69, 253
Ekers R.D., Fanti R., Lari C., Parma P., 1981, A&A 101, 194
Fanti R., Gioia I., Lari C., Ulrich M.H., 1978, A&AS 34, 341
Fanti C., Fanti R., de Ruiter H.R., Parma P., 1987, A&A 69, 57
Feretti L., Perola G.C., Fanti R., 1992, A&A 265, 9
Feretti L., Giovannini G., Klein U., et al., 1998, A&A 331, 475
Jaffe W.J., Perola G.C., 1974, A&A 26, 423
Jägers W.J., 1981, Ph.D. Thesis, Leiden University
Kardashev N.S., 1962, Sov. Astron. 6, 317
Katz-Stone D.M., Rudnick L., 1994, ApJ 426, 116
Katz-Stone D.M., Rudnick L., Anderson M.C., 1993, ApJ 407, 544
Kellermann K.I., 1964, ApJ 140, 969
Klein U., Mack K.-H., Gregorini L., Parma P., 1995, A&A 303, 427
Klein U., Mack K.-H., Gregorini L., Parma P., 1996, The Relic Radio Source B2 0924+30. In: Ekers R., Fanti C., Padrielli L.(eds.) Proc. IAU Symp. 175, Extragalactic Radio Sources. Kluwer Academic Publisher, p. 345
Leahy J.P., Muxlow T.W., Stephens P.W., 1989, MNRAS 239, 401
Liu R., Pooley G.G., Riley J.M., 1992, MNRAS 257, 545
Mack K.-H., Klein U., O'Dea C.P., Willis A.G., Saripalli L., 1998, A&A 329, 431
Massaglia S., Bodo G., Ferrari A., 1996, A&A 307, 997
Morganti R., Fanti C., Fanti R., Parma P., de Ruiter H., 1987, A&A 183, 203
Morganti R., Fanti R., Gioia I.M., et al., 1988, A&A 189, 11
Morganti R., Parma P., Capetti A., et al., 1997a, A&AS 126, 335
Morganti R., Parma P., Capetti A., Fanti R., de Ruiter H.R., 1997b, A&A 326, 919
Murgia M., 1996, Laurea Thesis, Univ. of Bologna
Myers S.T., Spangler S.R., 1985, ApJ 291, 52
Norman M.L., 1993, Numerical Simulation of Astrophysical Jets. In: Burgarella D, Livio M., O'Dea C. (eds.) Proc. of the Astrophysical Jets Meeting, Astrophysical Jets. Cambridge Univ. Press, p. 211
Pacholczyk A.G., 1970, Radio astrophysics. Freeman, San Francisco
Parma P., Ekers R.D., Fanti R., 1985, A&AS 59, 511
Parma P., de Ruiter H.R., Mack K.-H., et al., 1996, A&A 311, 49
Rudnick L., Katz-Stone D.M., Anderson M.C., 1994, ApJS 90, 955
Scheuer P.A.G., 1982, Morphology and Power of Radio Sources. In: Heeschen D., Wade C. (eds.) Proc. IAU Symp. No. 197, Extragalactic Radio Sources. D. Reidel Publishing Co., p. 163
Scheuer P.A.G., 1995, MNRAS 277, 331
van der Laan H., Perola G.C., 1969, A&A 3, 468